Journal of Organometallic Chemistry 694 (2009) 3892–3901

Contents lists available at ScienceDirect

Journal of Organometallic Chemistry

journal homepage: www.elsevier.com/locate/jorganchem

Palladium(II) and platinum(II) complexes of β-functionalized ethyl selenolates: Effect of substitution on synthesis, reactivity, spectroscopy, structures and thermal behavior

Liladhar B. Kumbhare [a], Amey P. Wadawale [a], Vimal K. Jain [a,*], Siddharth Kolay [b], Munirathinam Nethaji [b]

[a] Chemistry Division, Bhabha Atomic Research Centre, Mumbai 400 085, India
[b] Department of Inorganic and Physical Chemistry, Indian Institute of Science, Bangalore 560 012, India

ARTICLE INFO

Article history:
Received 2 June 2009
Received in revised form 3 August 2009
Accepted 4 August 2009
Available online 8 August 2009

Keywords:
Palladium
Platinum
β-Substituted ethylselenolate
X-ray structures
NMR spectroscopy

ABSTRACT

Sodium ethylselenolates with functional groups X (where X = –OH, –COOH, –COOMe and –COOEt) at β-carbon were prepared *in situ* by reductive cleavage of corresponding diselenide with $NaBH_4$ either in methanol or aqueous ammonia. Treatment of these selenolates with $[M_2Cl_2(\mu\text{–}Cl)_2(PR'_3)_2]$ (M = Pd or Pt; PR'_3 = $PMePh_2$, $PnPr_3$) in different stoichiometry yielded various bi- and tri-nuclear complexes. The homoleptic hexanuclear complexes $[Pd(\mu\text{–}SeCH_2CH_2X)_2]_6$ (X = OH, COOH, COOEt), were obtained by reacting Na_2PdCl_4 with $NaSeCH_2CH_2X$. All these complexes have been fully characterized. Molecular structures of ethylselenolates containing hydroxyl and carboxylic acid groups revealed solid state associated structures through inter-molecular hydrogen bond interactions. Trinuclear complex, $[Pd_3Cl_2(\mu\text{–}SeCH_2CH_2COOH)_4(PnPr_3)_2]$ (**3a**), was disposed in a boat form unlike chair conformation observed for the corresponding methylester complex. The effect of β-functionality in ethylselenolate ligands towards reactivity, structures and thermal properties of palladium and platinum complexes has been extensively studied.

1. Introduction

The chemistry of platinum group metal chalcogenolate complexes has been an active area of research for the past several decades [1–3] and has been dominated by complexes containing M–SR linkages. The varied applications in several areas such as catalysis [4–9], enzymatic models in biological systems, in cancer chemotherapy [10,11] and more recently as molecular precursors for metal chalcogenides, M_xE_y (M = Pd or Pt; E = S, Se, and Te) [12–14] have been a motivating factor for the sustained interest in these complexes.

The chemistry of metal chalcogenolates, keeping other factors unchanged (like metal and/or chalcogen atoms, auxiliary ligands on metal), is greatly influenced by the nature of R group attached to chalcogen. Thus various structural motifs have been identified when R group is changed from simple alkyl/aryl to bulky aryl (e.g., (2,4,6-$C_6H_2R_3$)E) [15] to internally functionalized R groups (e.g., 2-pyE, E = S, Se, Te) [16–18]. For instance, reactions of $[M_2Cl_2(\mu\text{–}Cl)_2(PR'_3)_2]$ with NaEPh in 1:2 molar ratio yield binuclear complexes, $[M_2Cl_2(\mu\text{–}EPh)_2(PR'_3)_2]$ whereas reactions with NaEpy under similar conditions give mononuclear complexes, $[MCl(Epy)(PR'_3)]$ (E = Se or Te) [17,18]. Internally functionalized ligands usually employ a neutral donor, like O, N, P, etc. and often serve as hemilabile ligands, finding relevance in homogeneous catalysis [6,19]. The chemistry of internally functionalized protic ligands, particularly with heavier chalcogen atoms, is rather scanty. The presence of protic groups may result in hydrogen bonding consequently forming self assembled metal–organic-frameworks showing different topologies. The design of metal–organic-frameworks utilizing the self assembly of molecules which contain complementary hydrogen bonding groups (e.g., *trans*-[$PdCl_2$(nicotinic acid)$_2$] [20]) has been well documented [20–24]. In the above perspective and in pursuance of our work on palladium and platinum chalcogenolates, we have examined the reactions of β-functionalized ethylselenolates with palladium and platinum complexes. Results of this work are described herein.

2. Results and discussion

2.1. Synthesis and spectroscopy

$^{77}Se\{^1H\}$ NMR chemical shift for sodium ethylselenolates, $NaSeCH_2CH_2X$ with various β-substitutions were in the order X = OH (−224 ppm) < COOH (−153 ppm) < COOEt (−148 ppm) < COOMe (−123 ppm). These values suggest that selenium site of hydroxyl derivative is the most electron rich. The diselenides followed the same order of chemical shift values as above, although,

* Corresponding author. Tel.: +91 22 2559 5095; fax: +91 22 2550 5151.
E-mail address: jainvk@barc.gov.in (V.K. Jain).

0022-328X/$ - see front matter © 2009 Elsevier B.V. All rights reserved.
doi:10.1016/j.jorganchem.2009.08.005

selenium resonance is significantly deshielded as compared to that of the corresponding selenolate [25].

Complexes, $[M_2Cl_2(\mu\text{–}SeR)_2(PR'_3)_2]$ (**1**), $[M_2Cl_2(\mu\text{–}Cl)(\mu\text{–}SeR)\text{-}(PR'_3)_2]$ (**2**) and $[Pd_2(SeR)_2(\mu\text{–}SeR)_2(PnPr_3)_2]$ (**4**) were isolated as yellow to orange-red crystalline solids by treatment of $[M_2Cl_2(\mu\text{–}Cl)_2(PR'_3)_2]$ (M = Pd or Pt; R = $Se(CH_2)_2OH$, $Se(CH_2)_2\text{-}COOH$, $Se(CH_2)_2COOMe$, $Se(CH_2)_2COOEt$; $PR'_3 = PMe_2Ph$, $PnPr_3$) with sodium selenolates in 1:2, 1:1 and 1:4 stoichiometry, respectively. The ^1H and ^{31}P NMR spectra revealed that **1** exists either as *sym-cis* or a mixture of *sym-cis* and *-trans* isomers with the predominance of the former which is appearing at lower frequencies. The *sym-trans* isomer when left in solution for several days, could convert into the *sym-cis* forms. The ^{77}Se and ^{195}Pt NMR spectra of **1** for acid and ester derivatives exhibited similar patterns and were as expected [26]. ^{77}Se NMR spectra were comprised of two sets of resonances for *cis* and one set of signals for *trans* isomer whereas, ^{195}Pt NMR spectra exhibited one set of resonances for each isomer with phosphorus-selenium/platinum couplings. However, the complexes containing $HOCH_2CH_2Se^-$ (**1a**–**1c**), two sets of resonances in ^{77}Se and ^{195}Pt NMR spectra of the *trans* isomer were observed suggesting that both the metal as well as bridging selenolates are magnetically nonequivalent in the *trans* isomer. The ^{77}Se signal showed pronounced metal (Pd or Pt) and phosphine dependence. The magnitude of various couplings, $^1J(^{195}Pt\text{–}^{31}P)$, $^2J(^{77}Se\text{–}^{31}P)_{cis/trans}$, $^2J(^{195}Pt\text{–}^{195}Pt)$, $^1J(^{195}Pt\text{–}^{77}Se)$ for **1** are in accordance with the reported values for organochalcogenolate bridged complexes [26,27–31]. The ^{31}P and ^{77}Se NMR spectra of **2** displayed single resonances indicating the formation of *sym-cis* isomer exclusively.

During the preparation of **1**, trinuclear $[Pd_3Cl_2(\mu\text{–}SeR)_4(PnPr_3)_2]$ (**3**) and binuclear tetrakis(selenolato) complex (**4**) were also formed, the latter two complexes could be separated from **1** by recrystallization. When the reaction of $[Pd_2Cl_2(\mu\text{–}Cl)_2(PnPr_3)_2]$ with more than 2.8 mol of $NaSeCH_2CH_2X$ was carried out, several binuclear complexes along with major product **1** (Scheme 1) were formed which could be identified by ^{31}P NMR spectroscopy. Intensities of ^{31}P NMR peaks suggest that **3** and $[Pd_2(\mu\text{–}SeR)_2\text{-}(PnPr_3)_4]\cdot 2Cl$ (**5**) were formed in appreciable quantity in the case of complexes containing $–SeCH_2CH_2COOR$ (R = H or Me) whereas hydroxyl derivative furnished **3** as a minor product. As is evident from ^{31}P NMR spectra, complex **4** was the major product for the latter, while it was the minor product for the former selenolates (Supplementary, Fig. 1). These observations could be explained with the fact that $^-SeCH_2CH_2OH$ is a stronger ligand in comparison of $^-SeCH_2CH_2COOR$ (R = H or Me) as supported by ^{77}Se chemical shifts. Thus the higher nucleophilic hydroxyl ligand replaces terminal chloride from $[Pd_2Cl_2(\mu\text{–}Cl)_2(PnPr_3)_2]$ with an ease leading to the substantial formation of **4**.

The complexes, **4** and $[Pd_2(\mu\text{–}SeR)_2(PnPr_3)_4]^{2+}$ (**5′**) (**5′** was traced by ^{31}P NMR spectroscopy without isolating it and hence its counter ion could not be ascertained) could also be obtained by transformation of $[Pd(SeR)_2(PnPr_3)_2]$ (**6**) in $CDCl_3$ solution

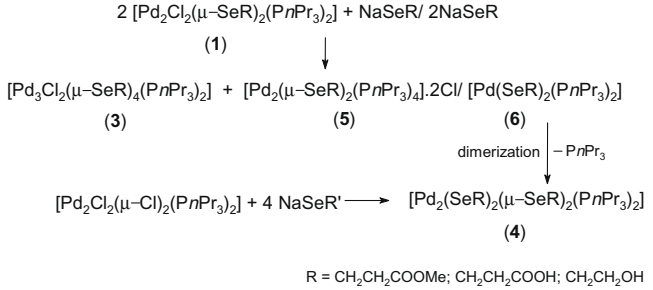

Scheme 1.

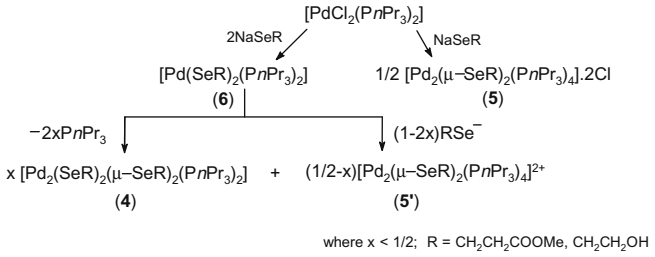

Scheme 2.

(Scheme 2). This transformation was monitored by time dependent ^{31}P NMR spectroscopy. For a given ligand, the formation of **4** against **5′** was hastened by purging air into a $CDCl_3$ solution, as conversion of phosphine to phosphine oxide drives formation of **5′** in forward direction (Fig. 1). Comparison of rate of formation of **5′** from **6** for hydroxyl and methyl ester functionalities clearly demonstrates the effect of β-substitution (Fig. 2). The concentration of $[Pd_2(\mu\text{–}SeCH_2CH_2OH)_2(PnPr_3)_4]^{2+}$ (**5′b**) grew faster as compared to $([Pd_2(\mu\text{–}SeCH_2CH_2COOMe)_2(PnPr_3)_4]^{2+}$ (**5′a**) which is attributed to the fact that higher nucleophilic hydroxyl selenolate must act as a poor leaving group. Therefore the conversion of **6** to **5′b** slows down while the growth of **4b** is accelerated as compared to that in the case of methyl ester derivative. The diminished growth rate for **4b** at longer standing time may be due to the formation of an insoluble complex having analytical data corresponding to $[Pd(\mu\text{–}SeCH_2CH_2OH)_2]_n$. This can be further supported by

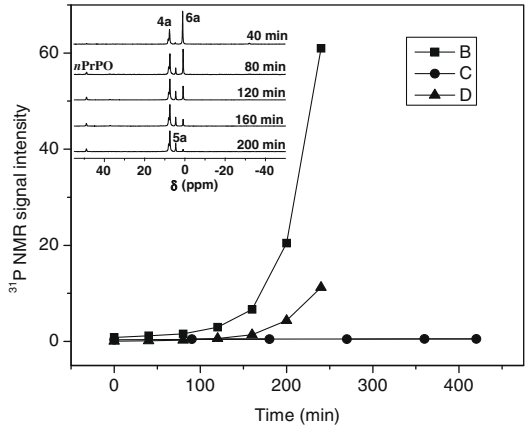

Fig. 1. Time trace of ^{31}P NMR intensity (the complexes containing $SeCH_2CH_2\text{-}COOMe$) with reference to **6a** for (B) **4a**, (D) **5a** when air was bubbled into the $CDCl_3$ solution; (C) **4a** without air bubbling. Inset ^{31}P NMR spectra for the conversion of **4a**– **5a** at different time when the air bubbled into the $CDCl_3$ solution.

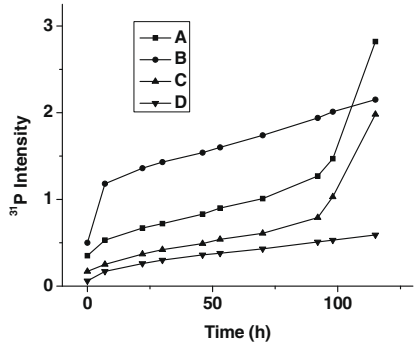

Fig. 2. Time traces of ^{31}P NMR signal intensities with reference to **6b** for (A) **4a**, (B) **4b** (C) **5b** (D) **5a** in $CDCl_3$.

increasing intensity of tripropylphosphine oxide signal in ^{31}P NMR spectra.

The homoleptic complexes, $[Pd(\mu\text{–}SeCH_2CH_2X)_2]_6$ (**7**), could be synthesized by the reaction of Na_2PdCl_4 with NaSeR. The yield of complexes depends upon their solubility in organic solvents. Ester derivatives being more soluble were obtained in the highest yield. The ^{77}Se and ^{13}C NMR spectra of **7** showed two sets of resonances for bridging selenolates, indicating existence of two different dispositions of selenolates with respect to hexagonal ring, one was within the ring plane and another being parallel to the ring axis. This was further confirmed by X-ray crystallography in which two slightly different Pd–Se bond distances have been observed (see later). Earlier, the existence of other oligomeric forms in solution was proposed for $[Pd(SeCH_2CH_2COOMe)_2]_6$ [26] based on the observation of two ^{77}Se NMR signals. Since the relative ratio of intensities of two sets in the ^{77}Se and ^{13}C NMR spectra does not vary by changing the ligand, existence of other oligomeric species in the solution may be ruled out.

2.2. Crystal structures

Molecular structures of $[Pd_2Cl_2(\mu\text{–}SeCH_2CH_2OH)_2(PMePh_2)_2]$ (**1b**), $[Pd_2Cl_2(\mu\text{–}SeCH_2CH_2COOH)_2(PMePh_2)_2]$ (**1e**), $[Pd_2Cl_2(\mu\text{–}Cl)(\mu\text{–}SeCH_2CH_2OH)(PMePh_2)_2]$ (**2a**), $[Pd_2Cl_2(\mu\text{–}Cl)(\mu\text{–}SeCH_2CH_2COOH)(PnPr_3)_2]$ (**2b**), $[Pd_3Cl_2(\mu\text{–}SeCH_2CH_2COOH)_4(PnPr_3)_2]$ (**3a**) and $[Pd(\mu\text{–}SeCH_2CH_2OH)_2]_6$ (**7a**) have been established unambiguously by X-ray crystallography. Selected bond lengths and angles are given in Tables 1–4. Figs. 3–8 (A), show ORTEP drawings with crystallographic numbering schemes and (B) show line diagram depicting short contacts and H-bondings (Supplementary Table 1) which are discussed on case by case basis. The C–Se distances in all these complexes lie in the region 1.955(9)–2.015(14) Å and are well within the range reported for the bridging organoselenolate ligands [31,32]. The Pd–Pd separations in all these complexes range between 3.176(1) and 3.401(1) Å which are significantly too long to account for any Pd–Pd bonding.

The complexes **1b** and **1e** comprise of two distorted square planar palladium atoms bridged together by two selenolato groups. The molecules adopt a *sym-cis* configuration with non-planar four-membered Pd_2Se_2 rings in which SeR ligands are exocyclic exhibiting an *anti* conformation. The Pd–Se distances *trans* to phosphine are longer (by ~0.1 Å) than those *trans* to chloride owing to the strong *trans* influence of the phosphine ligands. The two Pd–Se distances are well within the range reported for palladium selenolate complexes [14,32,33]. The Pd–P and Pd–Cl distances are as expected [32,34]. The Se–Pd–Se angles (~81°), similar in two molecules, are significantly smaller than the ideal value of 90° indicating strain in the four-membered Pd_2Se_2 ring. Although the

Table 1
Selected bond lengths (Å) and bond angles (°) for $[Pd_2Cl_2(\mu\text{–}SeCH_2CH_2OH)_2(PMePh_2)_2]$ (**1b**) and $[Pd_2Cl_2(\mu\text{–}SeCH_2CH_2COOH)_2(PMePh_2)_2]$ (**1e**).

1b		**1e**	
Pd1–P1	2.282(1)	P1–Pd1	2.281(3)
Pd1–P2	2.291(1)	P2–Pd2	2.290(3)
Pd1–Se2	2.396(1)	Pd1–Se2	2.472(1)
Pd1–Se1	2.474(1)	Pd1–Se1	2.403(1)
Pd2–Se2	2.386(1)	Pd2–Se2	2.463(1)
Pd2–Se1	2.482(1)	Pd2–Se1	2.402(1)
Cl1–Pd1	2.348(1)	Cl1–Pd1	2.362(3)
Cl2–Pd2	2.346(1)	Cl2–Pd2	2.383(3)
C14–Se1	1.976(4)	C1–Se1	1.995(10)
C16–Se2	1.967(5)	C4–Se2	1.990(9)
C15–O1	1.245(7)	C3–O1	1.242(13)
C17–O2	1.408(7)	C3–O2	1.318(12)
Pd1–Pd2	3.317(1)	C6–O3	1.222(12)
		C6–O4	1.317(12)
		Pd1–Pd2	3.401(1)
P1–Pd1–Cl1	88.42(4)	P1–Pd1–Cl1	90.37(11)
P1–Pd1–Se2	93.30(3)	P1–Pd1–Se2	174.71(9)
Cl1–Pd1–Se2	173.16(4)	Cl1–Pd1–Se2	94.76(8)
P1–Pd1–Se1	175.11(3)	P1–Pd1–Se1	94.00(9)
Cl1–Pd1–Se1	96.44(3)	Cl1–Pd1–Se1	174.36(9)
Se2–Pd1–Se1	81.81(2)	Se2–Pd1–Se1	80.97(5)
P2–Pd2–Cl2	88.89(4)	P2–Pd2–Cl2	90.86(10)
P2–Pd2–Se2	95.09(3)	P2–Pd2–Se2	173.64(8)
Cl2–Pd2–Se2	170.87(3)	Cl2–Pd2–Se2	94.10(7)
P2–Pd2–Se1	171.78(3)	P2–Pd2–Se1	93.96(8)
Cl2–Pd2–Se1	95.27(4)	Cl2–Pd2–Se1	175.04(8)
Se2–Pd2–Se1	81.84(2)	Se2–Pd2–Se1	81.17(5)
C14–Se1–Pd1	107.06(15)	C1–Se1–Pd1	99.1(3)
C14–Se1–Pd2	108.67(16)	C1–Se1–Pd2	102.3(3)
Pd1–Se1–Pd2	84.05(2)	Pd1–Se1–Pd2	90.10(5)
C16–Se2–Pd2	103.77(16)	C4–Se2–Pd2	107.6(3)
C16–Se2–Pd1	106.02(15)	C4–Se2–Pd1	108.6(3)
Pd2–Se2–Pd1	87.86(2)	Pd2–Se2–Pd1	87.10(5)

Table 2
Selected bond lengths (Å) and bond angles (°) for $[Pd_2Cl_2(\mu\text{–}Cl)(\mu\text{–}SeCH_2CH_2OH)(PMePh_2)_2]\cdot CHCl_3$ (**2a**) and $[Pd_2Cl_2(\mu\text{–}Cl)(\mu\text{–}SeCH_2CH_2COOH)(PnPr_3)_2]$ (**2b**).

2a		**2b**	
Pd1–Se1	2.375(2)	Cl1–Pd1	2.413(2)
Pd1–Cl3	2.431(4)	Cl1–Pd2	2.419(2)
Pd1–P1	2.230(4)	Cl2–Pd1	2.334(2)
Pd1–Cl1	2.347(4)	Cl3–Pd2	2.329(2)
Pd2–Se1	2.392(2)	P1–Pd1	2.233(2)
Pd2–Cl3	2.428(3)	P2–Pd2	2.233(2)
Pd2–P2	2.227(4)	Pd1–Se1	2.393(1)
Pd2–Cl2	2.336(4)	Pd2–Se1	2.386(1)
Se1–C28	2.015(14)	C19–Se1	1.975(9)
O1–C27	1.428(18)	O2–C21	1.294(11)
Pd1–Pd2	3.270(2)	C21–O1	1.209(11)
		Pd1–Pd2	3.212(1)
Pd1–Se1–Pd2	86.61(7)	P1–Pd1–Cl2	88.69(9)
Pd1–Cl3–Pd2	84.60(11)	P1–Pd1–Se1	93.77(6)
Se1–Pd1–Cl3	85.69(10)	Cl2–Pd1–Se1	175.84(8)
Se1–Pd2–Cl3	85.39(10)	P1–Pd1–Cl1	177.27(8)
Se1–Pd1–P1	92.56(11)	Cl2–Pd1–Cl1	92.50(8)
Cl3–Pd1–Cl1	92.78(13)	Se1–Pd1–Cl1	84.91(5)
Se1–Pd1–Cl1	177.15(10)	P2–Pd2–Cl3	88.38(9)
P1–Pd1–Cl1	89.01(14)	P2–Pd2–Se1	94.03(6)
P1–Pd1–Cl3	178.03(14)	Cl3–Pd2–Se1	174.94(8)
Se1–Pd2–P2	89.92(11)	P2–Pd2–Cl1	177.29(9)
Cl3–Pd2–Cl2	93.16(14)	Cl3–Pd2–Cl1	92.87(9)
Se1–Pd2–Cl2	174.99(11)	Se1–Pd2–Cl1	84.92(5)
P2–Pd2–Cl3	175.28(13)	C19–Se1–Pd2	100.9(2)
Pd1–Se1–C28	99.5(6)	C19–Se1–Pd1	102.5(3)
Pd2–Se1–C28	100.3(5)	Pd2–Se1–Pd1	84.44(3)
P2–Pd2–Cl2	91.46(14)	Pd1–Cl1–Pd2	83.33(6)

Table 3
Selected bond lengths (Å) and bond angles (°) for $[Pd_3Cl_2(\mu\text{–}SeCH_2CH_2COOH)_4(PnPr_3)_2]$ (**3a**).

P1–Pd2	2.278(3)	C1–Se1	1.966(10)
Cl1–Pd2	2.344(3)	C4–Se2	1.967(9)
Pd1–Se2	2.426(1)	C3–O1	1.227(13)
Pd1–Se1	2.433(1)	C3–O2	1.228(14)
Pd2–Se2	2.484(1)	C6–O3	1.144(17)
Pd2–Se1	2.402(1)	C6–O4	1.241(17)
Pd1–Pd2	3.176(1)		
P1–Pd2–Cl1	89.15(12)	Se2[a]–Pd1–Se1	97.51(4)
P1–Pd2–Se1	93.84(9)	Se2–Pd1–Se1[a]	97.51(4)
Cl1–Pd2–Se2	95.40(8)	Se1–Pd1–Se1[a]	169.65(7)
Se2–Pd2–Se1	81.63(5)	Se2–Pd1–Se2[a]	176.99(7)
P1–Pd2–Se2	175.45(9)	C1–Se1–Pd2	102.3(3)
Cl1–Pd2–Se1	175.32(9)	Pd1–Se1–C1	105.9(3)
Pd2–Se1–Pd1	82.12(4)	C4–Se2–Pd2	109.5(3)
Pd2–Se2–Pd1	80.58(4)	Pd1–Se2–C4	109.0(3)
Se1–Pd1–Se2	82.21(4)	Pd2–Pd1–Pd2[a]	110.10(5)

[a] Denotes symmetrical moiety with respect to centre of inversion.

Table 4
Selected bond lengths (Å) and bond angles (°) for $[Pd(\mu\text{–}SeCH_2CH_2OH)_2]_6$ (**7a**).

Pd1–Se2	2.446(1)	Pd3–Se6	2.445(1)
Pd1–Se5[i]	2.442(1)	Pd1–Pd2	3.186(1)
Pd1–Se6	2.439(1)	Pd2–Pd3	3.263(1)
Pd1[i]–Se5	2.442(1)	Pd3–Pd1[i]	3.227(1)
Pd2–Se1	2.441(1)	Se1–C1	1.955(9)
Pd2–Se2	2.449(1)	Se2[i]–C3	1.970(8)
Pd2–Se3	2.430(1)	Se3–C5	1.978(8)
Pd2–Se4	2.448(1)	Se4–C7	1.972(8)
Pd3–Se3	2.440(1)	Se5–C9	1.960(8)
Pd3–Se4	2.446(1)	Se6–C11	1.987(9)
Pd3–Se5	2.426(1)		
Se1–Pd1–Se2	81.92(4)	Se3–Pd3–Se4	83.38(4)
Se1–Pd1–Se5[i]	179.33(4)	Se3–Pd3–Se6	174.14(4)
Se1–Pd1–Se6[i]	96.77(4)	Se5–Pd3–Se3	97.06(4)
Se5[i]–Pd1–Se2	98.73(4)	Se5–Pd3–Se4	178.18(4)
Se6[i]–Pd1–Se2	175.36(4)	Se5–Pd3–Se6	82.79(4)
Se6[i]–Pd1–Se5[i]	82.60(4)	Se6–Pd3–Se4	96.95(4)
Se1–Pd2–Se2	81.55(4)	Pd1–Se1–Pd2	81.79(3)
Se1–Pd2–Se4	178.81(4)	Pd1–Se2–Pd2	81.20(4)
Se3–Pd2–Se1	96.83(4)	Pd2–Se3–Pd3	84.15(4)
Se3–Pd2–Se2	173.73(4)	Pd3–Se4–Pd2	83.63(4)
Se3–Pd2–Se4	83.57(4)	Pd3–Se5–Pd1[i]	83.02(4)
Se4–Pd2–Se2	97.93(4)	Pd1[i]–Se6–Pd3	82.70(4)

[i] Denotes symmetrical moiety with respect to centre of inversion.

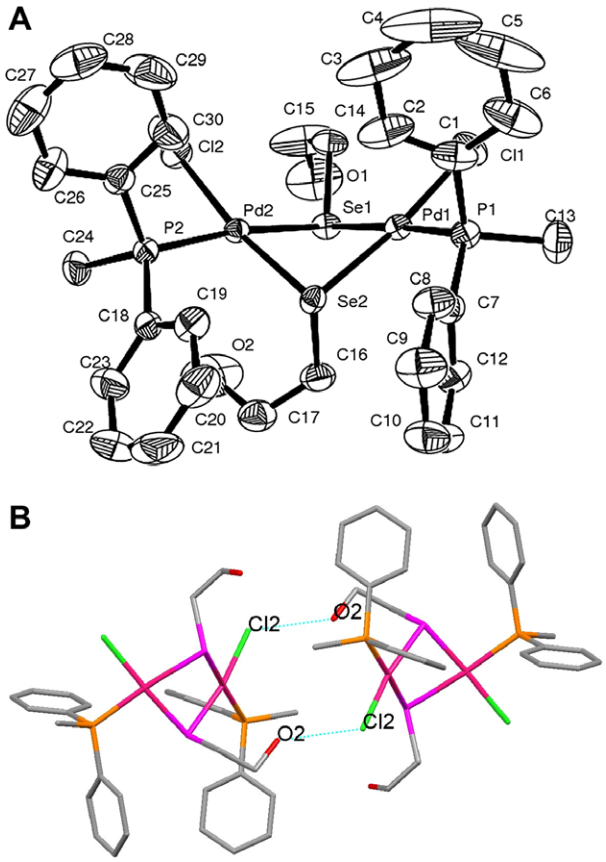

Fig. 3. (A) ORTEP diagram of *cis*-$[Pd_2Cl_2(\mu\text{–}SeCH_2CH_2OH)_2(PMePh_2)_2]$ (**1b**) (ellipsoids drawn with 50% probability); (B) line diagram showing short contacts (hydrogen atoms are omitted for clarity).

Pd(1)–Se(2)–Pd(2) (bridging selenolate *trans* to phosphine) are essentially similar in both the complexes, the angle Pd(1)–Se(1)–Pd(2) (bridging selenolate *trans* to chloride) are significantly different (84.05 (2)° for **1b** and 90.10 (5)° for **1e**).

The core at the metal centres of **2a** and **2b** are isomorphous. The dimeric molecules have two distorted square planar palladium atoms sharing bridging chloride and selenolate ligands, forming a non-planar, four-membered "Pd_2SeCl" ring. The molecules adopt a *sym-cis* configuration with phosphine ligands *trans* to bridging chloride. The Pd–Se distances for the two complexes are similar and are comparable with other selenolato-bridged palladium derivatives [14,33]. The Pd–$Cl_{(bridging)}$ distances are longer (by ~0.1 Å) than the corresponding values for Pd–$Cl_{(terminal)}$ although these distances are within the range reported for chloro-bridged binuclear palladium complexes [35,36]. The Se–Pd–Cl angles (~85°) are all similar in two complexes which have opened up slightly from Se–Pd–Se angles in bis(selenolato)-bridged complexes, **1b** and **1e** (~81°). The hydroxyl group of bridging selenolate ligands in binuclear complexes **1b** and **2a** show interaction with the terminal chloride (Cl···O = 3.037(7) Å for **1b** and 3.096(1) Å for **2a**) of the inversion related molecules resulting in dimeric molecular assemblies. The carboxylic acid groups of bridging selenolate ligands in **1e** and **2b** of centrosymmetrically related molecules showed hydrogen bonding interactions (O···O = 2.613(15) and 2.636(13) Å for **1e** and 2.696(5) Å for **2b**). In the former selenolate groups are intermolecularly hydrogen bonded to inversion related molecules to form an infinite polymeric chain of binuclear Pd complexes.

The structure of **3a** consists of three square planar palladium atoms sharing four bridging selenolato groups. The molecule has a boat shape (Scheme 3) and represents the first example of such a conformation for complexes having "$M_3(\mu\text{–}ER)_4$" core. For instance, complexes, $[Pd_3Cl_2(\mu\text{–}SHx)_4(PMe_3)_2]$ [37], $[Pt_3(\mu\text{–}Stol)_4(dppm)_2][CF_3SO_3]_2$ [38], $[Pd_3(\mu\text{–}SMes)_4(\eta^3\text{–}C_4H_7)_2]$ [33], $[Pd_3Cl_2(\mu\text{–}SeCH_2CH_2COOMe)_4(PnPr_3)_2]$ [26] have a zigzag shape. Thus the boat conformation in **3a** may be attributed to the stabilization due to hydrogen bonding. The central palladium atom (Pd1) in **3a** is surrounded by Se_4 core with essentially similar Pd–Se distances. The coordination environment around terminal palladium atoms is defined by two bridging selenolates, a chloride and a phosphine ligand. The central palladium atom is at the inversion centre of the molecule. The Pd–Pd distances (3.176 (1) Å) are smaller than those reported for $[Pd_3Cl_2(\mu\text{–}SeCH_2CH_2COOMe)_4(PnPr_3)_2]$ [26]. The various bond lengths and angles in "$PdClPdSe_2$" fragment are similar to the one observed for **1b** and **1e**. The R groups on bridging Se atoms in "$Pd(SeR)_2$" fragment adopt an *anti* configuration. Each molecule has a series of OH···O=C contacts (Fig. 7B) viz. O2···O4 = 2.642(1), O1···O3 = 2.655(1) and O4···O4 = 2.998(1) (Å) with its neighbours leading to a supramolecular aggregation. The carboxylic acid groups of bridging selenolate of one side of molecule **a** interacts with the carboxylic acid groups of another molecule **b** while the carboxylic acid group on other side of the molecule **a** coordinates with –COOH group of molecule **c.** Typical O···O distances in carboxylic acid derivatives have been reported to be 2.637(3) Å [19].

The homoleptic complex **7a** is hexameric comprising of a centrosymmetric Pd_6Se_{12} hexagon in which each square planar palladium atoms has a $PdSe_4$ core. The two adjacent palladium atoms are held together by two selenolato bridges. The palladium coordination planes are inclined to each other by 64.35°, 56.55° and 59.10° (coordination planes of Pd1 and Pd2, Pd2 and Pd3, and Pd1 and Pd3, respectively) resulting into a Pd_6Se_{12} hexagon. As a consequence of formation of hexagon, the Se–Pd–Se angles around each palladium atom are split into acute (~82°, within the ring plane) and obtuse (~98°, parallel to the ring axis) sets. In "$Pd_2(SeCH_2CH_2OH)_2$" fragment, the Pd–Se distances originating from one of the bridging selenolate groups are slightly longer than the other bridging ligand, although all the Pd–Se distances (2.430(1)–2.448(1) Å) lie within the range reported for selenolate complexes [14,32,33,36]. The overall structure is isomorphous to

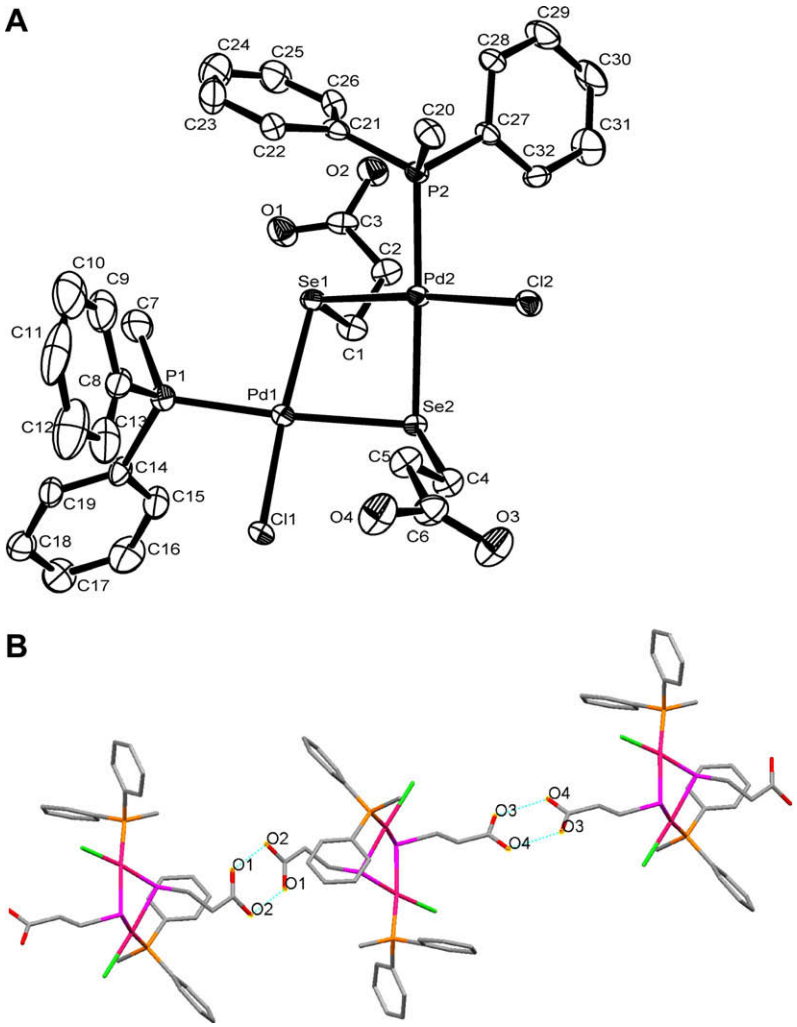

Fig. 4. (A) ORTEP diagram of *cis*-$[Pd_2Cl_2(\mu\text{–}SeCH_2CH_2COOH)_2(PMePh_2)_2]$ (**1e**) (ellipsoids drawn with 25% probability); (B) line diagram showing H-bridges (hydrogen atoms are omitted for clarity).

$[Pd(\mu\text{–}SeCH_2CH_2X)_2]_6$ (X = NMe_2 [36], COOMe [26]) and $[Pd(SR)_2]_6$ (R = *n*Pr [39,40], CH_2COOMe [41]). There are several intermolecular OH···O hydrogen bonding contacts (O2···O5 = 2.730(12), O2···O6 = 2.717(10), O3···O4 = 2.559(15), O3···O5 = 2.706(16), O1···O6 = 2.716(12), O1···O4 = 2.686(15) Å). Each OH group is hydrogen bonded to its nearest oxygen atom of neighbouring molecule. Such interactions lead to the formation of a 3D array of hexameric Pd_6Se_{12} core. Packing of **7a** (Fig. 8B) shows extensive network of intermolecular hydrogen bonds with channel down the *a*-axis of diameters 7.542 and 6.887 Å.

2.3. Thermal studies

TG curves for **1a, 1g** and $[Pd_2Cl_2(\mu\text{–}SeCH_2CH_2COOMe)_2(PnPr_3)_2]$ (Supplementary, Fig. 3) showed weight loss of 58.2 (Calc. 58.6)% at 202 °C, 64.1 (Calc. 63.5)% at 265 °C and 62.7 (Calc. 62.4)% at 248 °C, respectively (parentheses indicate weight loss corresponding to the formation of $Pd_{17}Se_{15}$). The observed weight loss indicates that these complexes, irrespective of β-substitution on ethylselenolate, decompose to $Pd_{17}Se_{15}$. However, β-substitution did influence the decomposition temperature. The complex **1a** decomposed at much lower temperature (202 °C) as compared to those derived from –$SeCH_2CH_2COOR$ (R = Me, Et). To prepare sufficient quantities of palladium selenide, complexes were pyrolyzed in a furnace at the corresponding decomposition temperature. The residues obtained were characterized by powder XRD which were consistent with the formation of $Pd_{17}Se_{15}$. The broadening of XRD pattern in case of **1a** (Supplementary, Fig. 3) suggests the formation of nanoparticles which may be favoured by low decomposition temperature. Decomposition byproducts of **1a** were analyzed by Q-MS coupled with TG. Mass spectra displayed oxygen bearing fragments (Supplementary, Fig. 4) at around 119 °C suggesting fragmentation of selenolate moiety. At 169 °C hydrocarbon fragments of relatively higher intensities were observed due to fragmentation of phosphine groups as well as some secondary fragmentation. Major fragments obtained from **1a** were H_2O, C_2H_4, C_2H_3 and C_2H_2.

3. Experimental

3.1. Materials and methods

The complexes, Na_2PdCl_4 and $[M_2Cl_2(\mu\text{–}Cl)_2(PR'_3)_2]$ (M = Pd, Pt; PR'_3 = $PMePh_2$, $PnPr_3$) and the ethyldiselenide $(\text{–}SeCH_2CH_2COOMe)_2$ were prepared according to literature methods [26,42]. All the reactions were carried out under an argon atmosphere in dry and distilled solvents. Microanalyses were carried out on a Carlo Erba EA-1110 CHN-O instrument. ^1H and proton decoupled ^{13}C, ^{31}P, ^{77}Se and ^{195}Pt NMR spectra were recorded in $CDCl_3$ on a Bruker Avance-II 300 MHz NMR spectrometer, operating at 300, 75.47, 121.49, 57.24 and 64.52 MHz, respectively. Chemical shifts (in

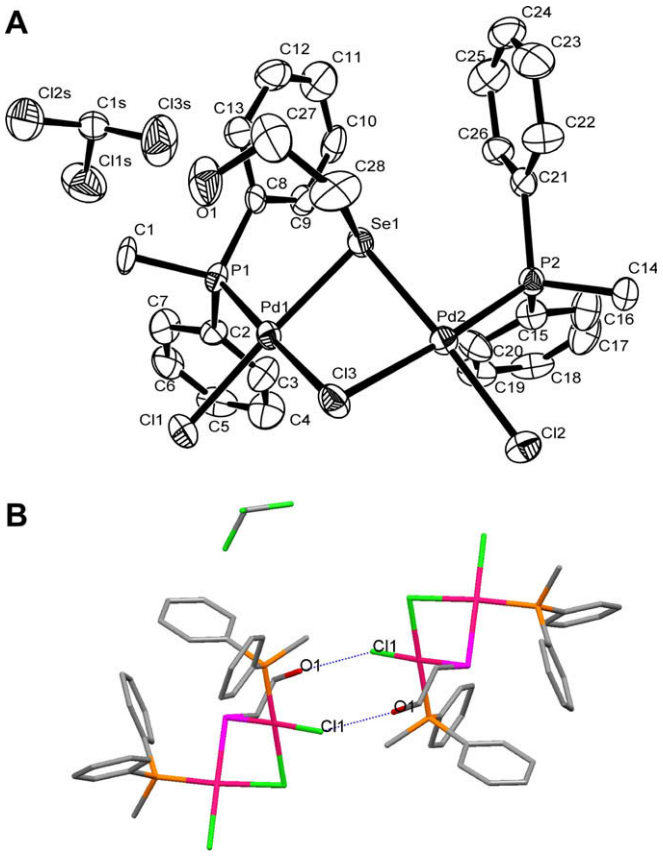

Fig. 5. (A) ORTEP diagram of *cis*-$[Pd_2Cl_2(\mu\text{–}Cl)(\mu\text{–}SeCH_2CH_2OH)(PMePh_2)_2]\cdot CHCl_3$ (**2a**) (ellipsoids drawn with 50% probability); (B) line diagram showing short contacts (hydrogen atoms are omitted for clarity).

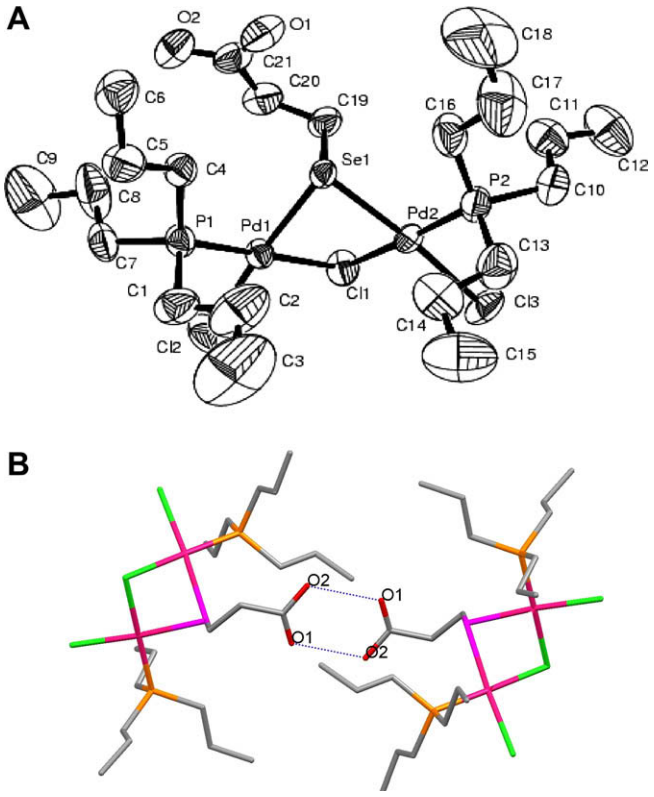

Fig. 6. (A) ORTEP diagram of *cis*-$[Pd_2Cl_2(\mu\text{–}Cl)(\mu\text{–}SeCH_2CH_2COOH)(PnPr_3)_2]$ (**2b**) (ellipsoids drawn with 50% probability); (B) line diagram showing H-bridges (hydrogen atoms are omitted for clarity).

ppm) are relative to TMS for ^1H and ^{13}C and external 85% H_3PO_4 for ^{31}P, Me_2Se for ^{77}Se (secondary reference Ph_2Se_2, δ 463 ppm) and Na_2PtCl_6 in D_2O for ^{195}Pt. For the time dependent ^{31}P NMR studies, freshly prepared $[Pd(SeCH_2CH_2COOMe)_2(PnPr_3)_2]$ (**6a**) (25 mg) in 6 mL of $CDCl_3$ was taken in a NMR tube. The spectra were recorded at a time interval, the first spectrum was designated as zero time spectrum. To the above solution, air was introduced intermittently for 30 min using a bubbler. The same procedure was repeated for **6b**. Mass spectra were recorded on a Waters Q-Tof micro (YA-105) time of flight mass spectrometer. TG curves with mass spectra were obtained under an argon atmosphere with a heating rate of 10 °C/min on SETARAM Setsys evolution-1750 TG analyzer coupled with **'**Quadstar 32-bit quadruple mass spectrometer**'**. Palladium selenides were obtained under a flow of argon by heating each of the complexes, (**1a**, **1g** and $[Pd_2Cl_2(\mu\text{–}SeCH_2CH_2COOMe)_2(PnPr_3)_2]$) in a glass tube housed in a furnace. Temperature of the furnace was set at 10 °C above the respective decomposition temperature obtained from TG curve.

3.2. Preparation of ligands

Bis(2-hydroxyethyl)diselenide, $(-SeCH_2CH_2OH)_2$ was synthesized by acid hydrolysis of corresponding potassium selenosulfate which was prepared by reacting aqueous potassium selenosulfate with ethanolic 1-bromoethanol [43,44]. The yellow oil obtained from this reaction was purified by column chromatography using 5% methanol in $CHCl_3$. Yield = 45%. Anal. Calc. for $C_4H_{10}O_2Se_2$: C, 19.4; H, 4.1. Found: C, 19.2; H, 4.0%. ^1H NMR ($CDCl_3$): δ 2.64 (s, 2H, OH); 3.11 (t, 7.7 Hz, 4H, $SeCH_2$); 3.92 (t, 7.7 Hz, 4H, OCH_2). ^{13}C NMR ($CDCl_3$): δ 32.6 [C–Se; $^1J(^{77}Se–^{13}C)$ = 75 Hz], 61.8 (C–O). ^{77}Se NMR ($CDCl_3$): δ 259.

3,3′-Diselenodipropionic acid, $(-SeCH_2CH_2COOH)_2$ was prepared from aqueous sodium diselenide and 2-bromopropionic acid [45]. Anal. Calc. for $C_6H_{10}O_4Se_2$: C, 23.7; H, 3.3. Found: C, 23.6; H, 3.4%. ^1H NMR (acetone-d_6): δ 2.79 (t, 7.0 Hz, 4H, $SeCH_2$); 3.11 (t, 6.8 Hz, 4H, $COOCH_2$); 4.26 (br, 2H, COOH). ^{13}C NMR (acetone-d_6): δ 23.4 [$^1J(^{77}Se–^{13}C)$ = 74 Hz], CH_2–Se), 35.2 (CH_2–O), 172.8 (COOH). ^{77}Se NMR (acetone-d_6): δ 325. Mass spectral data (m/e): 304 [M^+], 287 [M–OH].

$(-SeCH_2CH_2COOEt)_2$ was synthesized by esterification of $(-SeCH_2CH_2COOH)_2$ with dry ethanol in the presence of concentrated sulfuric acid. Anal. Calc. for $C_{10}H_{18}O_4Se_2$: C, 33.3; H, 5.0. Found: C, 33.1; H, 4.7%. ^1H NMR ($CDCl_3$): δ 1.23 (t, 7.2 Hz, 6H, OCH_2CH_3); 2.78 (t, 7.1 Hz, 4H, $SeCH_2$); 3.06 (t, 7.2 Hz, 4H, $COOCH_2$); 4.12 (q, 7.2 Hz, 4H, OCH_2). ^{13}C NMR ($CDCl_3$): δ 14.2 (OCH_2CH_3); 23.3 [$^1J(^{77}Se–^{13}C)$ = 75 Hz, CH_2Se]; 35.9 (CH_2CO), 60.7 (OCH_2), 172.1 (COO). ^{77}Se NMR ($CDCl_3$): δ 324.

3.3. Synthesis of palladium(II) and platinum(II) complexes

3.3.1. $[Pd_2Cl_2(\mu\text{–}SeCH_2CH_2OH)_2(PnPr_3)_2]$ (**1a**)

To a freshly prepared methanolic solution of $NaSeCH_2CH_2OH$ (prepared *in situ* by the reaction of $(-SeCH_2CH_2OH)_2$ (119 mg, 0.48 mmol) with $NaBH_4$ (36 mg, 0.96 mmol) in anhydrous methanol), a dichloromethane solution of $[Pd_2Cl_2(\mu\text{–}Cl)_2(P^nPr_3)_2]$ (308 mg, 0.46 mmol) was added with vigorous stirring which continued for 1 h. The resulting orange solution was evaporated under vacuum and the residue was extracted with dichloromethane and filtered. The filtrate was reduced to 5 mL and layered by a mixture of ethylacetate and hexane. The solution on cooling in a freezer gave orange crystalline solid of the title complex (200 mg, 64%). m.p. 108–110 °C. ^1H NMR ($CDCl_3$): δ 1.07 (t), 1.63 (m), 1.86 (m) [$PnPr_3$]; 2.89 (t), 3.32 (m) (each OCH_2); 3.94 ($SeCH_2$); 4.14 (br,

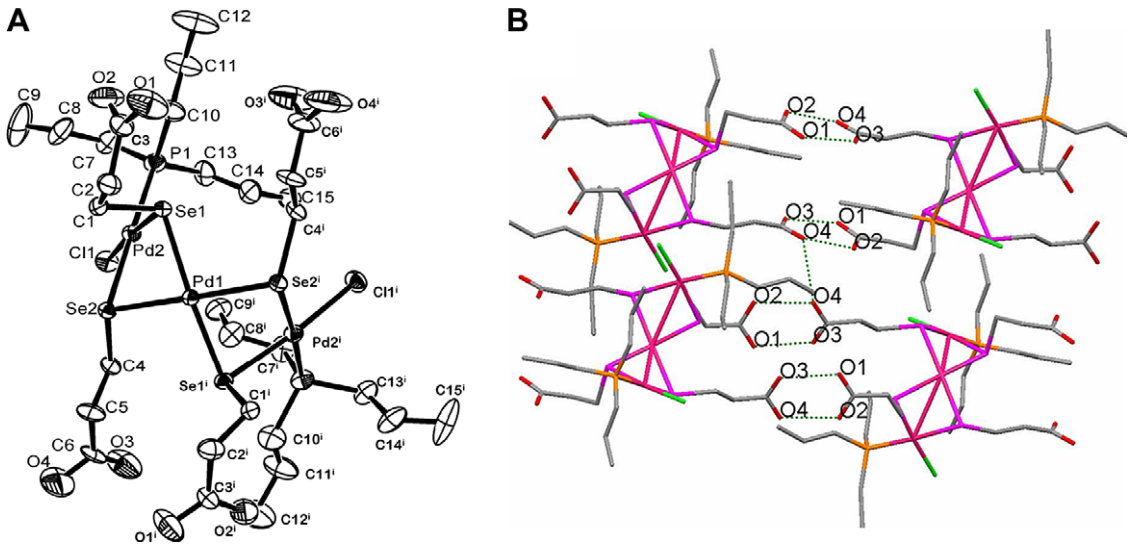

Fig. 7. (A) ORTEP diagram of *trans*-$[Pd_3Cl_2(\mu\text{–}SeCH_2CH_2COOH)_4(PnPr_3)_2]$ (**3a**) (ellipsoids drawn with 25% probability); (B) line diagram showing H-bridges (hydrogen atoms are omitted for clarity).

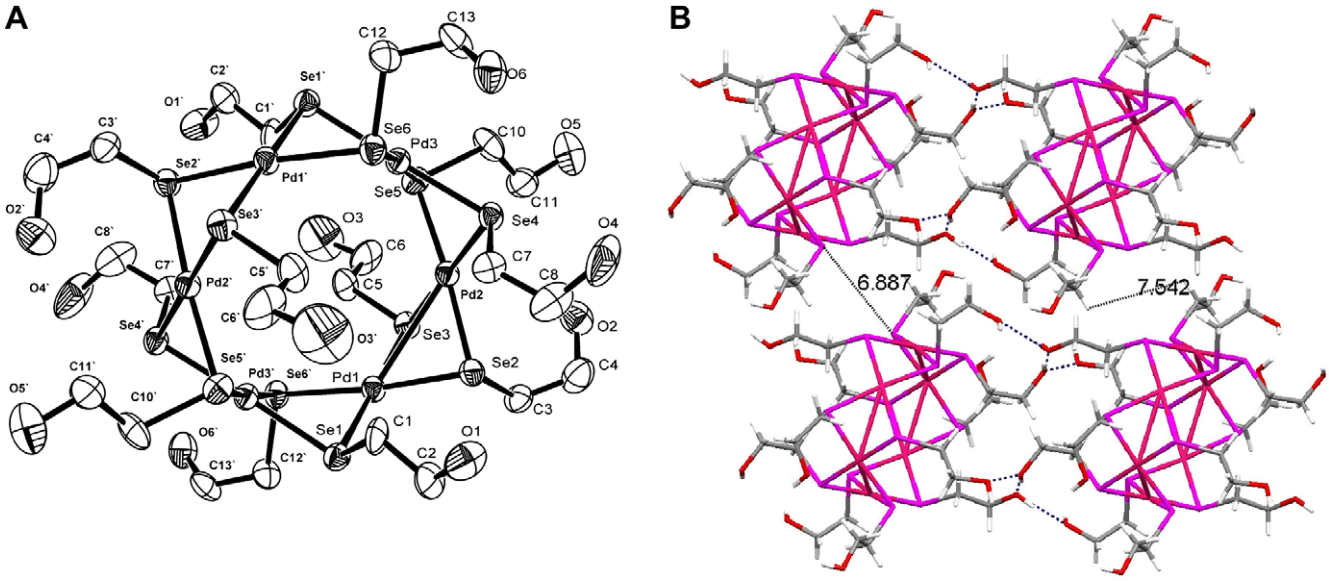

Fig. 8. (A) ORTEP diagram of $[Pd(\mu\text{–}SeCH_2CH_2OH)_2]_6$ (**7a**) (ellipsoids drawn with 50% probability); (B) line diagram showing H-bridges (hydrogen atoms are omitted for clarity).

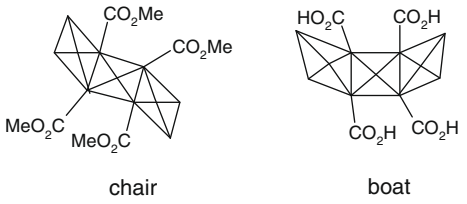

Scheme 3. Schematic representation of conformations for trinuclear palladium complex.

OH). $^{31}P\{^1H\}$ NMR ($CDCl_3$: δ 13.6 (s, *cis*); 14.2 (s, *trans*). $^{77}Se\{^1H\}$ NMR ($CDCl_3$): δ −74 (SeR *trans* to Cl); −92 [t, $^2J(^{77}Se–^{31}P) = 133$ Hz), SeR *trans* to $PnPr_3$] [*cis* isomer]. −315 (d, 139 Hz); −397 (d, 148 Hz) [*trans* isomer]. Anal. Calc. for $C_{22}H_{52}Cl_2O_2P_2Pd_2Se_2$: C, 31.0; H, 6.1. Found: C, 31.1; H, 6.1%.

3.3.2. $[Pd_2Cl_2(\mu\text{–}SeCH_2CH_2OH)_2(PMePh_2)_2]$ (**1b**)

Prepared similar to **1a** in 55% yield. m.p. 163–165 °C. ^1H NMR ($CDCl_3$): δ 2.10, 2.14 (each d, $^2J(^{31}P–^1H) = 12$ Hz, PMe); 3.14, 3.24, 3.48, 3.78 (br, $SeCH_2CH_2$ from *cis* and *trans* isomers); 4.05 (br, OH); 7.33–7.71 (m, PPh_2). $^{31}P\{^1H\}$ NMR ($CDCl_3$): δ 8.7 (*cis* isomer), 10.1 (*trans* isomer). $^{77}Se\{^1H\}$ NMR $CDCl_3$: δ −15 (SeR *trans* to Cl); −67 [t, $^2J(^{77}Se–^{31}P) = 139$ Hz], SeR *trans* to $PMePh_2$] [*cis isomer*]. −217 (d, 146 Hz); −227 (d, 146 Hz) [*trans* isomer]. Anal. Calc. for $C_{30}H_{36}Cl_2O_2P_2Pd_2Se_2$: C, 38.6; H, 3.9. Found: C, 38.7; H, 3.8%.

3.3.3. $[Pt_2Cl_2(\text{-}SeCH_2CH_2OH)_2(PnPr_3)_2]$ (**1c**)

Title complex was prepared analogous to **1a**. m.p. 133–135 °C. ^1H NMR ($CDCl_3$): δ 1.05 (t), 1.60 (br) [$PnPr_3$]; 2.70 (t, *trans* isomer); 2.93 (t, *cis* isomer); 3.36 (br), 3.51 (br) (*trans* isomer) [each OCH_2]. 3.84 (t, *cis* isomer); 4.03 (t, *trans* isomer) [each $SeCH_2$]; 4.20 (br, OH). $^{31}P\{^1H\}$ NMR ($CDCl_3$): δ 0.5 [s, *cis* isomer, $^1J(^{195}Pt\ –^{31}P) = 3132$ Hz]; 0.9 [s, *trans* isomer, $^1J(^{195}Pt–^{31}P) = 3066$ Hz]. $^{77}Se\{^1H\}$

NMR ($CDCl_3$): δ −127 (br); −167 [$^1J(^{195}Pt–^{77}Se)$ = 244 Hz)] [*cis* isomer]. −296 (d, 145 Hz); −315 (d, 130 Hz) [*trans* isomer]. ^{195}Pt NMR ($CDCl_3$): δ −4058 [$^1J(^{195}Pt–^{31}P)$ = 3136 Hz; $^2J(^{195}Pt–^{195}Pt)$ = 925 Hz] [*cis* isomer]. −3840 [d, $^1J(^{195}Pt–^{31}P)$ = 3053 Hz]; −3918 [d, $^1J(^{195}Pt–^{31}P)$ = 3053 Hz] [*trans* isomer]. Anal. Calc. for $C_{22}H_{52}Cl_2O_2P_2Pt_2Se_2$: C, 25.7; H, 5.1. Found: C, 25.6; H, 4.8%.

3.3.4. $[Pd_2Cl_2(\mu–SeCH_2CH_2COOH)_2(PnPr_3)_2]$ (**1d**)

To a mixture of $(–SeCH_2CH_2COOH)_2$ (100 mg, 0.33 mmol) and $NaBH_4$ (37 mg, 0.99 mmol), ammonia solution (600 μL of 25%) in distilled water (2 cm^3) was added and the whole was stirred under an argon atmosphere. To this concentrated sulfuric acid (150 μL) was added followed by addition of an acetone solution of $[Pd_2Cl_2(\mu–Cl)_2(PnPr_3)_2]$ (210 mg, 0.31 mmol). The reaction mixture was stirred for 1 h at room temperature. The solvents were evaporated under vacuum and the residue was washed with water, dried under vacuum and extracted with dichloromethane and filtered. The filtrate was concentrated to 5 mL and layered with hexane–acetone mixture, which on refrigeration afforded orange crystals of the title complex (yield 60%). m.p. 135 °C. ^1H NMR ($CDCl_3$): δ 1.08 (t), 1.61 (br), 1.88 (br) [$PnPr_3$]; 2.81, 2.87 (br, $SeCH_2$), 3.14, 3.20 (br, CH_2, *syn* and *anti*), 4.77 (br, OH). $^{31}P\{^1H\}$ NMR (acetone-d_6): δ 13.8 (*cis* isomer)14.5 (*trans* isomer). $^{77}Se\{^1H\}$ NMR (acetone-d_6): δ −51 (SeR *trans* to Cl); −70 [(t, $^2J(^{77}Se–^{31}P)$ = 137 Hz, *trans* to $PnPr_3$] [*cis* isomer]. Anal. Calc. for $C_{24}H_{52}Cl_2O_4P_2Pd_2Se_2$: C, 31.7; H, 5.8. Found: C, 31.6; H, 5.6%.

3.3.5. $[Pd_2Cl_2(\mu\text{-}SeCH_2CH_2COOH)_2(PMePh_2)_2]$ (**1e**)

Prepared similar to **1d** (yield 54%). m.p. 185 °C. ^1H NMR ($CDCl_3$): δ 2.10, 2.20 (each d, PMe); 2.45, 2.88, 3.13, 3.18, 3.44 (each t, $SeCH_2CH_2$); 7.30–7.85 (m, PPh_2). $^{31}P\{^1H\}$ NMR (acetone-d_6): δ 8.6 (*cis* isomer), 10.3 (*trans* isomer). $^{77}Se\{^1H\}$ NMR (acetone-d_6): δ −24 (SeR *trans* to Cl); −35 [t, $^1J(^{77}P–^{77}Se)$ = 141 Hz, SeR *trans* to $PMePh_2$] [*cis* isomer]. Anal. Calc. for $C_{32}H_{36}Cl_2O_4P_2Pd_2Se_2$: C, 38.9; H, 3.7. Found: C, 38.7; H, 4.0%.

3.3.6. $[Pt_2Cl_2(\mu–SeCH_2CH_2COOH)_2(PnPr_3)_2]$ (**1f**)

Prepared similar to **1d** (yield 50%). m.p. 192–194 °C. ^1H NMR ($CDCl_3$): δ 1.07 (t), 1.60 (br), 1.85 (br) [$PnPr_3$]; 2.77, 2.92, 3.24, 3.34 (each br, $SeCH_2CH_2$); 4.33 (br, COOH). $^{31}P\{^1H\}$ NMR (acetone-d_6): δ −1.0 [$^1J(^{195}Pt–^{31}P)$ = 3168 Hz; $^2J(^{195}Pt–^{195}Pt)$ = 916 Hz) (*cis* isomer). $^{77}Se\{^1H\}$ NMR (acetone-d_6): δ −92 ($^1J(^{195}Pt–^{77}Se)$ = 153 Hz); −131 [$^1J(^{195}Pt–^{77}Se)$ = 252 Hz [*cis* isomer]. $^{195}Pt\{^1H\}$ NMR (acetone-d_6): δ −4059 (d, $^1J(^{195}Pt–^{31}P)$ = 3174 Hz; $^2J(^{195}Pt–^{195}Pt)$ = 924 Hz] [*cis* isomer]. Anal. Calc. for $C_{24}H_{52}Cl_2O_4P_2Pt_2Se_2$: C, 26.5; H, 4.8. Found: C, 26.3; H, 4.6%.

3.3.7. $[Pd_2Cl_2(\mu–SeCH_2CH_2COOEt)_2(PnPr_3)_2]$ (**1g**)

Prepared similar to **1a** (yield 65%). m.p. 100–101 °C. ^1H NMR ($CDCl_3$): δ 1.08 (t), 1.60 (br), 1.82–1.91 (m) [$PnPr_3$];1.23, 1.28 (each t, 7 Hz, CH_2Me); 2.78, 2.86 ($SeCH_2$); 3.04 (t), 3.23 (br) (CH_2CO); 4.12, 4.15 (each q, OCH_2). $^{31}P\{^1H\}$ NMR ($CDCl_3$): δ 12.8 (s, *cis* isomer); 13.2 (4%, *trans* isomer). $^{77}Se\{^1H\}$ NMR ($CDCl_3$): δ −62 [$^2J(^{77}Se–^{31}P)$ = 134 Hz, *trans* to PPr_3]; −70 (*trans* to Cl) [*cis* isomer]; −257 [d, $^2J(^{77}Se–^{31}P)$ = 152 Hz, ∼5%] [*trans* isomer]. Anal. Calc. for $C_{28}H_{60}Cl_2O_4P_2Pd_2Se_2$: C, 34.9; H, 6.3. Found: C, 34.8; H, 6.5%.

3.3.8. $[Pd_2Cl_2(\mu–Cl)(\mu–SeCH_2CH_2OH)(PMePh_2)_2]$ (**2a**)

Prepared in a similar manner to **1a** by the reaction between $[Pd_2Cl_2(\mu–Cl)_2(PMePh_2)_2]$ (264 mg, 0.35 mmol) and $NaSeCH_2CH_2OH$ [prepared *in situ* from $(–SeCH_2CH_2OH)_2$ (90 mg, 0.36 mmol) with $NaBH_4$ (28 mg, 0.73 mmol) in absolute methanol] and recrystallized from dichloromethane-hexane as a yellow crystalline solid (yield, 200 mg, 68%). m.p. 206–207 °C. ^1H NMR ($CDCl_3$): δ 2.07 (t, 2 H, OCH_2); 2.23 [d, 12 Hz, 6H, PMe]; 3.64 (br, 2 H, $SeCH_2$); 7.30–7.80 [m, Ph]. $^{31}P\{^1H\}$ NMR ($CDCl_3$): δ 22.5. Anal. Calc. for $C_{28}H_{21}Cl_3OP_2Pd_2Se$: C, 39.9; H, 3.7. Found: C, 39.7; H, 3.6%.

3.3.9. $[Pd_2Cl_2(\mu–Cl)(\mu–SeCH_2CH_2COOH)(PnPr_3)_2]$ (**2b**)

Prepared analogous to complex **1d** from $[Pd_2Cl_2(\mu–Cl)_2(PnPr_3)_2]$ (375 mg, 0.56 mmol) and $NaSeCH_2CH_2COOH$ (prepared from $NaBH_4$ (21 mg, 0.60 mmol), $(–SeCH_2CH_2COOH)_2$ (83 mg, 0.30 mmol), ammonia solution (0.2 ml of 25%), conc. H_2SO_4 (0.05 ml) in water) in 1:1 molar ratio and the resulting complex was recrystallized from chloroform (yield 65%). m.p. 200–202 °C. ^1H NMR ($CDCl_3$): δ 1.07–1.11 (m), 1.78 (br) [$PnPr_3$]; 2.90, 3.01, 3.17, 3.36 (each t, $SeCH_2CH_2$). $^{31}P\{^1H\}$ NMR ($CDCl_3$): δ 32.2. $^{77}Se\{^1H\}$ NMR ($CDCl_3$): δ 35. Anal. Calc. for $C_{21}H_{47}Cl_3O_2P_2Pd_2Se$: C, 31.9; H, 6.0. Found: C, 32.3; H, 5.9%. When $[Pd_2Cl_2(\mu–Cl)_2(PnPr_3)_2]$ was treated with $NaSeCH_2CH_2COOH$ in methanol in order to prepare diselenido complex (**1d**), complex **2b** was obtained instead, due to incomplete cleavage of diselenide by methanolic $NaBH_4$.

3.3.10. $[Pd_3Cl_2(\mu–SeCH_2CH_2COOH)_4(PnPr_3)_2]$ (**3a**)

This was isolated as a byproduct from **1d** during recrystallization in poor yield (∼8%). m.p. 200 °C. ^1H NMR ($CDCl_3$): δ 1.08, 1.62, 1.87 [$PnPr_3$]; 2.20, 2.88 ($SeCH_2CH_2$); 3.11 (t, COOH). $^{31}P\{^1H\}$ NMR ($CDCl_3$): δ 14.0 (*cis* isomer),15.7 (*trans* isomer). ^{77}Se $\{^1H\}$ NMR ($CDCl_3$): δ −52 [d, $^2J(^{77}Se–^{31}P)$ = 135 Hz, SeR *trans* to PR_3]; −96 (SeR *trans* to Cl) [*cis* isomer]. Anal. Calc. for $C_{30}H_{62}Cl_2O_8P_2Pd_3Se_4$: C, 27.3; H, 4.7. Found: C, 27.6; H, 4.6%.

3.3.11. $[Pd_2(SeCH_2CH_2OH)_2(\mu–SeCH_2CH_2OH)_2(PnPr_3)_2]$ (**4b**)

This complex was prepared in a manner similar to $[Pd_2(SeCH_2CH_2COOMe)_2(\mu–SeCH_2CH_2COOMe)_2(PnPr_3)_2]$ (**4a**) [26]. $^{31}P\{^1H\}$ NMR ($CDCl_3$): δ 7.9, 9.0.

3.3.12. $[Pd_2(\mu–SeCH_2CH_2COOMe)_2(PnPr_3)_4]Cl_2$ (**5a**)

Dichloromethane solution of $[PdCl_2(PnPr_3)_2]$ (220 mg, 0.44 mmol) was reacted with a methanolic solution of $NaSeCH_2CH_2COOMe$ (prepared *in situ* by the reaction of $(–SeCH_2CH_2COOMe)_2$ (74 mg, 0.22 mmol) with $NaBH_4$ (18 mg, 0.48 mmol) in anhydrous methanol), stirred for 15 min, filtered and dried under vacuum. ^1H NMR ($CDCl_3$): δ 0.95 (t), 1.46 (m), 1.85 (m) [$PnPr_3$]; 2.49–2.59 (m, $SeCH_2CH_2$); 3.58 (s, OMe). $^{31}P\{^1H\}$ NMR ($CDCl_3$): δ 4.6. $^{77}Se\{^1H\}$ NMR ($CDCl_3$): δ −31. Similarly $[Pd_2(\mu–SeCH_2CH_2OH)_2(PnPr_3)_4]Cl_2$ (**5b**) was prepared. $^{31}P\{^1H\}$ NMR ($CDCl_3$): δ 4.8.

3.3.13. $[Pd(SeCH_2CH_2COOMe)_2(PnPr_3)_2]$ (**6a**)

Prepared analogous to **5a**, from $[PdCl_2(PnPr_3)_2]$ (110 mg, 0.22 mmol), $(–SeCH_2CH_2COOMe)_2$ (81 mg, 0.24 mmol) and $NaBH_4$ (20 mg, 0.53 mmol). ^1H NMR ($CDCl_3$): δ 0.95 (t), 1.42 (br), 2.0 (br) [$PnPr_3$]; 2.50, 2.56 (each br, $SeCH_2CH_2$); 3.59 (s, OMe). $^{31}P\{^1H\}$ NMR ($CDCl_3$): δ 0.9. $^{77}Se\{^1H\}$ NMR ($CDCl_3$): δ −73. Similarly $[Pd(SeCH_2CH_2OH)_2(PnPr_3)_2]$ (**6b**) was prepared. $^{31}P\{^1H\}$ NMR ($CDCl_3$): δ 0.5. $^{77}Se\{^1H\}$ NMR ($CDCl_3$): δ −154.

3.3.14. $[Pd(\mu–SeCH_2CH_2OH)_2]_6$ (**7a**)

A methanolic solution of Na_2PdCl_4 (390 mg, 1.33 mmol) was added to a solution of $NaSeCH_2CH_2OH$ [prepared from $NaBH_4$ (100 mg, 2.63 mmol) and $(–SeCH_2CH_2OH)_2$ (329 mg, 1.33 mmol) in methanol] and stirred for 3 h under an argon atmosphere, whereupon a brown precipitate formed. The precipitate was filtered and extracted with ethanol. The solution was passed through cellite and concentrated under vacuum. The solution on slow evaporation afforded deep red crystals of the title complex (yield 40%). m.p. 258–260 °C. $^{13}C\{^1H\}$ NMR (dmso-d_6): δ 29.1, 26.3 (each s, $SeCH_2$), 62.0, 65.0 (each s, OCH_2). $^{77}Se\{^1H\}$ NMR (dmso-d_6): δ −68, −207. Anal. Calc. for $C_{24}H_{60}O_8Pd_6Se_{12}$: C, 13.5; H, 2.8. Found: C, 13.9; H, 2.6%.

Table 5
Crystal data and structure refinement details of $[Pd_2Cl_2(\mu\text{–}SeCH_2CH_2OH)_2(PMePh_2)_2]$ (**1b**), $[Pd_2Cl_2(\mu\text{–}SeCH_2CH_2COOH)_2(PMePh_2)_2]$ (**1e**), $[Pd_2Cl_2(\mu\text{–}Cl)(\mu\text{–}SeCH_2CH_2OH)_2(PMePh_2)_2]\cdot CHCl_3$ (**2a**), $[Pd_2Cl_2(\mu\text{–}Cl)(\mu\text{–}SeCH_2CH_2COOH)(PnPr_3)_2]$ (**2b**), $[Pd_3Cl_2(\mu\text{–}SeCH_2CH_2OH)_4(PnPr_3)_2]$ (**3a**) and $[Pd(\mu\text{–}SeCH_2CH_2OH)_2]_6$ (**7a**).

	1b	**1e**	**2a·CHCl$_3$**	**2b**	**3a**	**7a**
Chemical formula	$C_{30}H_{36}Cl_2O_2P_2Pd_2Se_2$	$C_{32}H_{36}Cl_2O_4P_2Pd_2Se_2$	$C_{29}H_{32}Cl_6OP_2Pd_2Se$	$C_{21}H_{47}Cl_3O_2P_2Pd_2Se$	$0.5(C_{30}H_{62}Cl_2O_8P_2Pd_3Se_4)$	$C_{24}H_{60}O_{12}Pd_6Se_{12}$
Formula weight	932.15	988.17	962.95	791.64	659.34	2126.64
Crystal size (mm^3)	0.37 × 0.32 × 0.29	0.30 × 0.10 × 0.10	0.10 × 0.10 × 0.10	0.43 × 0.32 × 0.30	0.3 × 0.15 × 0.15	0.20 × 0.20 × 0.20
Crystal system	Triclinic	Triclinic	Monoclinic	Monoclinic	Monoclinic	Triclinic
Space group	$P\bar{1}$	$P\bar{1}$	$P2_1/c$	$P2_1/n$	$C2/c$	$P\bar{1}$
Unit cell dimensions						
a (Å)	11.273(2)	11.723(3)	13.070(6)	13.2798(13)	16.700(5)	11.0797(14)
b (Å)	11.578(3)	13.600(4)	21.646(12)	18.5511(18)	21.393(8)	11.1000(12)
c (Å)	14.635(3)	13.888(9)	12.991(5)	14.5042(14)	14.978(4)	11.4471(15)
α (Å)	93.593(4)	107.90(3)				103.950(9)
β (Å)	109.687(3)	98.07(3)	103.04(3)	112.273(2)	115.52(2)	104.609(10)
γ (Å)	107.917(3)	110.920(18)				101.020(9)
Volume (Å^3)/Z	1681.6(6)/2	1888.5(14)/2	3581(3)/4	3306.6(6)/4	4829(3)/8	1273.7 (3)/1
μ (mm^{-1})/F (0 0 0)	3.514/912	3.139/968	2.581/1888	2.543/1584	4.335/2576	10.692/984
θ Range (°)	2.50–27.50	2.63–27.49	2.68–27.53	2.35–27.00	2.60–27.49	2.98–27.51
Limiting indices	$-15 \leqslant h \leqslant 15$ $-14 \leqslant k \leqslant 14$ $-19 \leqslant l \leqslant 18$	$-15 \leqslant h \leqslant 15$ $-16 \leqslant k \leqslant 17$ $-18 \leqslant l \leqslant 10$	$-9 \leqslant h \leqslant 16$ $0 \leqslant k \leqslant 28$ $-16 \leqslant l \leqslant 16$	$-17 \leqslant h \leqslant 17$ $-23 \leqslant k \leqslant 24$ $-19 \leqslant l \leqslant 17$	$-12 \leqslant h \leqslant 21$ $0 \leqslant k \leqslant 27$ $-19 \leqslant l \leqslant 17$	$-8 \leqslant l \leqslant 14$ $-14 \leqslant h \leqslant 14$ $-14 \leqslant k \leqslant 14$
Number of reflections/ unique	19723/7851	10346/8625	9836/8199	28369/7748	6614/5548	7045/ 5843
Number of data/ restraints/parameters	7851/0/365	8625/0/399	8199/0/370	7748/0/287	5548/0/222	5843/0/250
Final $R_1[I > 2\sigma(I)]$, ωR_2	0.0363, 0.0563	0.0582, 0.2307	0.0711, 0.1515	0.0451, 0.0763	0.0549, 0.0990	0.0417, 0.0823
R_1, ωR_2 (all data)	0.0811, 0.0887	0.0959, 0.1339	0.2662, 0.2130	0.0937, 0.0892	0.2119, 0.1357	0.1065, 0.0988
Goodness of fit on F^2	1.022	0.936	0.949	1.000	0.924	1.000

Measurement temperature = 298(2) K; X-ray wavelength = 0.71073 Å.

3.3.15. $[Pd(\mu\text{–}SeCH_2CH_2COOH)_2]_6$ (**7b**)

Prepared similar to **7a** in aqueous medium (yield 40%). m.p. 260–262 °C. $^{13}C\{^1H\}$ NMR (dmso-d_6): δ 18.2, 20.8 (each s, $SeCH_2$); 36.2, 39.0 (each s, $-CH_2-$); 172.7 (s, COOH). $^{77}Se\{^1H\}$ NMR (dmso-d_6): δ –34, –171. Anal. Calc. for $C_{36}H_{60}O_{24}Pd_6Se_{12}$: C, 17.5; H, 2.5. Found: C, 18.0; H, 2.5%.

3.3.16. $[Pd(\mu\text{–}SeCH_2CH_2COOEt)_2]_6$ (**7c**)

Prepared similar to **7a** in methanol (yield 65%). m.p. 104–106 °C. $^{13}C\{^1H\}$ NMR ($CDCl_3$): δ 14.2 (s, CH_3); 17.9, 20.7 (each s, $SeCH_2$); 36.4, 39.3 (each s, $-CH_2-$); 60.5, 60.7 (each s, OCH_2), 171.4 (s, C=O). $^{77}Se\{^1H\}$ NMR ($CDCl_3$): δ –36, –175. Anal. Calc. for $C_{60}H_{108}O_{24}Pd_6Se_{12}$: C, 25.7; H, 3.9. Found: C, 26.0; H, 3.6%.

3.4. X-ray crystallography

Unit cell parameters and intensity data for **1b** and **2b** were collected on a Bruker Smart Apex CCD diffractometer using Mo Kα radiation (λ = 0.71073 Å) employing the ω scan technique. The intensity data were corrected for Lorentz, polarization and absorption effects. The structures were solved and refined with SHELX program [46], non-hydrogen atoms were refined anisotropically. Intensity data for **1e**, **2a**, **3a** and 7**a** were collected on a Rigaku AFC7S diffractometer fitted with Mo Kα radiation so that θ_{max} = 27.5 Å. The structures were solved by direct methods [47] and refinement was on F^2 [46] using data which were corrected for absorption correction effects employing an empirical procedure [48,49]. The non-hydrogen atoms were refined with anisotropic displacement parameters and fitted with hydrogen atoms in their calculated positions. Molecular structures were drawn using ORTEP [50]. Crystallographic data and structural refinement details are given in Table 5.

4. Conclusions

Higher nucleophilicity of $HOCH_2CH_2Se^-$ has certain consequences vis-à-vis ester and acid analog such as decomposition temperature for conversion of $[Pd_2Cl_2(SeR)_2(PnPr_3)_2]$ to $Pd_{17}Se_{15}$ is lower, conversion of $[Pd(SeR)_2(PnPr_3)_2]$ to $[Pd_2(SeR)_2(\mu\text{–}SeR)_2(PnPr_3)_2]$ is faster. However, tendency to form trinuclear species is subdued for hydroxyl ligand compared to that of acid and ester derivatives. Presence of hydrogen bonding in solid state structures plays important role in stabilizing uncommon boat conformation.

Acknowledgements

Authors thank Drs T. Mukherjee and D. Das for encouragement of this work. We are thankful to the Chemistry Department, IIT Bombay, Mumbai for providing microanalysis and mass spectra of the complexes.

Appendix A. Supplementary data

CCDC 710910, 710911, 710912, 710913, 715043, and 715044 contain the supplementary crystallographic data for these compounds ($[Pd(\mu\text{–}SeCH_2CH_2OH)_2]_6$), ($[Pd_2Cl_2(\mu\text{–}Cl)(\mu\text{–}SeCH_2CH_2OH)(PMePh_2)_2CHCl_3]$), ($[Pd_3Cl_2(\mu\text{–}SeCH_2CH_2COOH)_4(PnPr_3)_2]$), ($[Pd_2Cl_2(\mu\text{–}SeCH_2CH_2COOH)_2(PMePh_2)_2]$), ($[Pd_2Cl_2(\mu\text{–}SeCH_2CH_2OH)_2(PMePh_2)_2]$), ($[Pd_2Cl_2(\mu\text{–}Cl)(\mu\text{–}SeCH_2CH_2COOH)(PnPr_3)_2]$). These data can be obtained free of charge from The Cambridge Crystallographic Data Centre via www.ccdc.cam.ac.uk/data_request/cif.

Supplementary data associated with this article can be found, in the online version, at doi:10.1016/j.jorganchem.2009.08.005.

References

[1] P.J. Blower, J.R. Dilworth, Coord. Chem. Rev. 76 (1987) 121.
[2] W. Levason, S.D. Orchard, Coord. Chem. Rev. 225 (2002) 159.
[3] W. Levason, Coord. Chem. Rev. 161 (1997) 33.
[4] L. Dong, S.B. Duckett, F.F. Ohman, W.D. Jones, J. Am. Chem. Soc. 114 (1992) 151.
[5] L.Y. Chiang, J.W. Skoirczewski, R. Kastrup, C.S. Hsu, R.B. Upasani, J. Am. Chem. Soc. 113 (1998) 6574.
[6] J.R. Dilworth, N. Wheatley, Coord. Chem. Rev. 119 (2000) 89.
[7] V.K. Jain, G.S. Rao, Inorg. Chim. Acta 127 (1987) 161.

[8] V.P. Ananikov, M.A. Kabeshov, I.P. Beletskaya, G.G. Aleksandrov, I.L. Eremenko, J. Organomet. Chem. 687 (2003) 651.
[9] V.P. Ananikov, M.A. Kabeshov, I.P. Beletskaya, V.N. Khrustalev, M.Yu. Antipin, Organometallics 24 (2005) 1275.
[10] B.P. Esposito, R. Najjar, Coord. Chem. Rev. 232 (2002) 137.
[11] J. Reedijk, Chem. Rev. 99 (1999) 2499.
[12] S. Dey, V.K. Jain, Platinum Metals Rev. 48 (2004) 16.
[13] L.B. Kumbhare, V.K. Jain, B. Varghese, Inorg. Chim. Acta 359 (2006) 409.
[14] S. Dey, V.K. Jain, S. Chaudhury, A. Knoedler, F. Lissner, W. Kaim, J. Chem. Soc., Dalton Trans. (2001) 723.
[15] J. Arnold, Prog. Inorg. Chem. 43 (1995) 353.
[16] E.S. Raper, Coord. Chem. Rev. 153 (1996) 199;
E.S. Raper, Coord. Chem. Rev. 165 (1997) 475.
[17] S. Narayan, V.K. Jain, B. Varghese, J. Chem. Soc., Dalton Trans. (1998) 2359.
[18] S. Dey, V.K. Jain, J. Singh, V. Trehan, K.K. Bhasin, B. Varghese, Eur. J. Inorg. Chem. (2003) 744.
[19] M.B. Smith, Platinum Metals Rev. 52 (2008) 215.
[20] Z. Qin, M.C. Jennings, R.J. Puddephatt, K.W. Muir, Inorg. Chem. 41 (2002) 5174.
[21] A.M. Beatty, Cryst. Eng. Commun. 51 (2001) 1.
[22] A.D. Burrows, C.W. Chan, M.M. Chowdhry, J.E. McGrady, D.M.P. Mingos, Chem. Soc. Rev. (1995) 329.
[23] A.M. Beatty, Coord. Chem. Rev. 246 (2003) 131.
[24] C.B. Aakeröy, A.M. Beatty, D.S. Leinen, Angew. Chem. Int. Ed. 38 (1999) 1815.
[25] H. Duddeck, Prog. Nucl. Mag. Res. Spectrosc. 27 (1995) 1.
[26] L.B. Kumbhare, V.K. Jain, P.P. Phadnis, M. Nethaji, J. Organomet. Chem. 692 (2007) 1546.
[27] V.K. Jain, L. Jain, Coord. Chem. Rev. 249 (2005) 3075.
[28] V.K. Jain, S. Kannan, R.J. Butcher, J.P. Jasinski, Polyhedron 14 (1995) 3641.
[29] V.K. Jain, S. Kannan, J. Organomet. Chem. 405 (1991) 265.
[30] V.K. Jain, S. Kannan, R.J. Butcher, J.P. Jasinski, J. Organomet. Chem. 468 (1994) 285.
[31] S. Dey, V.K. Jain, B. Varghese, J. Organomet. Chem. 623 (2001) 48.
[32] S. Dey, L.B. Kumbhare, V.K. Jain, T. Schurr, W. Kaim, A. Klein, F. Belaj, Eur. J. Inorg. Chem. (2004) 4510.
[33] N. Ghavale, S. Dey, A. Wadawale, V.K. Jain, Organometallics 27 (2008) 3297.
[34] V.K. Jain, S. Kannan, E.R.T. Tiekink, J. Chem. Soc., Dalton Trans. (1992) 2231.
[35] V.K. Jain, R.P. Patel, K.V. Muralidharan, R. Bohra, Polyhedron 8 (1989) 2151.
[36] S. Dey, V.K. Jain, A. Klein, W. Kaim, Inorg. Chem. Commun. 7 (2004) 601.
[37] E.M. Padilla, C.M. Jensen, Polyhedron 10 (1991) 89.
[38] A. Singhal, V.K. Jain, A. Klein, M. Niemeyer, W. Kaim, Inorg. Chim. Acta 357 (2004) 2134.
[39] N.R. Kunchur, Acta Crystallogr., Sect. B 24 (1968) 1623.
[40] J.D. Higgins-III, J.W. Suggs, Inorg. Chim. Acta 145 (1988) 247.
[41] L. Schneider, M. Hörner, R.N. Olendzki, J. Strähle, Acta Crystallogr., Sect. C 49 (1993) 2091.
[42] H.C. Clark, G. Ferguson, V.K. Jain, M. Parvez, Inorg. Chem. 24 (1985) 1477.
[43] A.P. Arnold, K.S. Tan, D.L. Rabenstein, Inorg. Chem. 25 (1986) 2433.
[44] K.S. Tan, A.P. Arnold, D.L. Rabenstein, Can. J. Chem. 66 (1988) 54.
[45] D.L. Klayman, T.S. Griffin, J. Am. Chem. Soc. 95 (1973) 197.
[46] G.M. Sheldrick, Acta Crystallogr. 64A (2008) 112.
[47] SIR-92, A. Altomare, G. Cascarano, C. Giacovazzo, A. Guagliardi, J. Appl. Cryst. 26 (1993) 343.
[48] T. Higashi, ABSCOR-Empirical Absorption Correction based on Fourier Series Approximation, Rigaku Corporation, 3-9-12 Matsubara, Akishima, Japan, 1995.
[49] PSISCANS-A. C.T. North, D.C. Phillips, F.S. Mathews, Acta Crystallogr., Sect. A 24 (1968) 351.
[50] C.K. Johnson, ORTEPII, Report ORNL-5136, Oak Ridge, National Laboratory, Oak Ridge, TN, 1976.